Improved Cell Search and Initial Synchronization Using PSS in LTE

Zhongshan Zhang†, Ming Lei‡, Keping Long† and Yong Fan⋆
†Institute of Advanced Network Technologies and New Services, University of Science and Technology Beijing (USTB), {zhangzs,longkeping}@ustb.edu.cn
‡Department of Wireless Communications, NEC Laboratories China (NLC), lei_ming@nec.cn
⋆Beijing LOIT Technology Ltd, fany@timeloit.com

***Abstract*— Cell search as well as synchronization in the 3rd Generation Partnership Project (3GPP) Long Term Evolution (LTE) system is performed in each User Equipment (UE) by using both the Primary Synchronization Signal (PSS) and Secondary Synchronization Signal (SSS), and the overall synchronization performance is dominated heavily by a robust PSS detection. Conventional non-coherent detector can achieve a reliable PSS detection based on the near-perfect auto-correlation and cross-correlation properties of Zadoff-Chu (ZC) sequences [1], but at the cost of a relatively high computational complexity. This paper proposes two improved PSS detectors, i.e., Almost Half-Complexity (AHC) and Central Self-Correlation (CSC) detectors, by exploiting the central-symmetric property of ZC sequences. The AHC detector has exactly the same detection accuracy as that of the conventional detector but with 50% complexity being saved, and the proposed CSC detector can further reduce its complexity to 50% that of the AHC detector, however, at a cost of a slight accurate degradation. In order to mitigate the potential failure risk due to a large frequency offset in the proposed algorithms while at the same time keep the PSS detection accuracy un-degraded, an improvement of CSC, i.e., CSC_{Ins}, is also proposed. The performance of CSC_{Ins} detector is independent of the frequency offset, and numerical results show that the 90% PSS acquisition time of CSC_{Ins} is well within a 55ms duration with Signal-to-Noise Ratio (SNR) of -10 dB.**

I. Introduction

The 3rd Generation Partnership Project (3GPP) Long Term Evolution (LTE) is envisioned to be a key technology for the next-generation wireless communications [2]. The LTE network, also known as Evolved Universal Terrestrial Radio Access Network (E-UTRAN), has been standardized by 3GPP [3].

In LTE, each cell is identified by the cell-ID information carried by both the Primary Synchronization Signal (PSS) and Secondary Synchronization Signal (SSS). A length-63 Zadoff-Chu (ZC) sequence, which occupies the central 6 Resource Blocks (RB) of the system bandwidth, is used to generate the PSS. The overall synchronization performance in LTE is dominated heavily by a robust PSS detection at User Equipments (UE). In [4], synchronization and cell search for 3GPP LTE systems based on the frequency-domain identification of PSS and SSS are discussed. A robust time and frequency synchronization scheme in 3GPP LTE is proposed in [5], where the Cyclic Prefix (CP)-based auto-correlation algorithm is first performed to identify the CP type and obtain the gross symbol synchronization at the same time, followed by the accurate synchronization achieved by detecting the PSS symbol.

However, all the algorithms aforementioned detect the PSS symbol by exploiting the near-perfect auto-correlation property of the ZC sequences, but this kind of non-coherent detection requires a full-length complex correlation between the received symbol and the local ZC sequence, and the computational burden is relatively high.

In this paper, improved PSS detection algorithms by exploiting the central-symmetric structure of the ZC sequences are studied. Two low-complexity detectors, i.e., the Almost-Half Complexity (AHC) detector and the Central Self-Correlation (CSC)-based PSS fast detector, are then proposed. A frequency offset independent detector, i.e., Frequency Offset Insensitive PSS Detection Based on the CSC Property (CSC_{Ins}), is also proposed to further improve the robustness of CSC detector. A local threshold is properly chosen in each algorithm based on the tradeoff between False-Alarm and Miss-Detection probabilities to enable a robust PSS detection, and the performance comparison among all these detectors is performed in terms of the 90% PSS acquisition time.

The remainder of this paper is organized as follows. A system model of PSS transmit & receive is provided in Section II, and the AHC detector is proposed in Section III. The CSC-based PSS fast detector is proposed in Section IV, followed by its improvement detector, i.e., CSC_{Ins}, being proposed in Section V. Performance of the proposed detectors is analyzed in Section VI, followed by numerical results given by Section VII. Finally, the conclusions are drawn in Section VIII[1].

II. System Signal Model

Three length-63 PSS sequences are used in LTE with each corresponding to one physical layer identify within each cell

[1]*Notation*: $(\cdot)^{-1}$, $(\cdot)^T$ and $(\cdot)^H$ are the inverse, transpose and complex conjugate transpose of a matrix. The imaginary unit is $\jmath = \sqrt{-1}$. A circularly symmetric complex Gaussian RV w with mean m and variance σ^2 is denoted by $w \sim \mathcal{CN}(m, \sigma^2)$. $\mathbf{0}_N$ is an $N \times 1$ all-zero vector. $\mathbf{a}[i]$ is the i-th entry of vector $\mathbf{a}$, and $\|\mathbf{a}\|_2^2 = \sum_i |\mathbf{a}[i]|^2$. $[\mathbf{B}]_{mn}$ is the mn-th entry of matrix $\mathbf{B}$. An $N \times N$ *Inverse Discrete Fourier Transform* (IDFT) matrix $\mathbf{F}$ is defined as $[\mathbf{F}]_{nk} = \frac{1}{\sqrt{N}} e^{\frac{\jmath 2\pi nk}{N}}$ for $0 \le n, k \le N-1$. $(x)_n$ represents the remainder after division of x by n. $\mathbb{E}\{x\}$ and $\text{Var}\{x\}$ are the mean and variance of x.

978-1-4673-0990-5/12/$31.00 ©2012 IEEE

group, as defined by

$$\mathrm{ZC}_M^{63}(n) = \exp\left[\frac{-\jmath\pi Mn(n+1)}{N_{ZC}}\right], \quad (1)$$

where $N_{ZC} = 63$, $n = 0, 1, \cdots, N_{ZC}-1$, and M is the ZC sequence root. For a given M, $\mathrm{ZC}_M^{63}(31)$ is not used to avoid modulating the d.c.-subcarrier, and the remaining 62 elements of this ZC sequence can be represented as

$$\mathbf{z}_M = [\mathrm{ZC}_M^{63}(0), \cdots, \mathrm{ZC}_M^{63}(30), 0, \mathrm{ZC}_M^{63}(32), \cdots, \mathrm{ZC}_M^{63}(62)]^T. \quad (2)$$

The evolved NodeB (eNodeB) broadcasts the PSS signal to its UEs once every 5ms period, and a UE performing the cell search will receive the DL frame and search the PSS signal symbol-by-symbol.

By using $h_{k,m}(z)$ to represent the discrete-time impulse response of the z-th tap channel between the m-th eNodeB and the k-th UE, the related channel response vector can be represented as $\mathbf{h}_{k,m} = [h_{k,m}(0), h_{k,m}(1), \cdots, h_{k,m}(L_{max}-1)]^T$ with L_{max} representing the maximum channel length. We also use an $N \times 1$ vector $\mathbf{x}_m$ to represent the PSS vector transmitted by the m-th eNodeB, where $\mathbf{x}_m = \left[\mathbf{0}_{\frac{N-62}{2}}, \mathbf{z}_M, \mathbf{0}_{\frac{N-64}{2}}\right]^T$ with N being the system's IDFT length.

The received base-band PSS vector in the k-th UE (we assume that the m-th eNodeB is the serving eNodeB of the k-th UE) is represented as

$$\mathbf{y}_k = \mathbf{E}_{k,m}\mathbf{F}\mathbf{H}_{k,m}\mathbf{x}_m + \sum_{z\in\Im_m} \mathbf{E}_{k,z}\mathbf{F}\mathbf{H}_{k,z}\mathbf{x}_z + \mathbf{w}_k, \quad (3)$$

where $\mathbf{H}_{k,l} = \mathrm{diag}\{H_{k,l}(0), H_{k,l}(1), \cdots, H_{k,l}(N-1)\}$ with $H_{k,l}(n) = \sum_{d=0}^{L_{max}-1} h_{k,l}(d)e^{-\frac{\jmath 2\pi nd}{N}}$, $\mathbf{E}_{k,l} = \mathrm{diag}\left\{1, e^{\frac{\jmath 2\pi\varepsilon_{k,l}}{N}}, \cdots, e^{\frac{\jmath 2\pi\varepsilon_{k,l}(N-1)}{N}}\right\}$ with $\varepsilon_{k,l}$ representing the normalized frequency offset (frequency offset normalized to a subcarrier spacing of OFDM symbols) between the k-th UE and the l-th eNodeB. $\Im_l$ represents the set of interfering eNodeBs of the l-th eNodeB. $\mathbf{w}_k$ is a vector of additive white Gaussian noise (AWGN) with $\mathbf{w}_k[i] \sim \mathcal{CN}(0, \sigma_w^2)$.

The detection of PSS requires the receiver to find the optimal M as well as the start position of the sequence (i.e., θ) to maximize the likelihood (Coherent Detection) or cross-correlation (Non-Coherent Detection) function between the transmit and receive sequences [2, Chapter 7.3]. Since the Coherent Detection requires the knowledge of channel state information, which is unavailable at the cell-search phase, we consider only the non-Coherent Detection in this paper[2]. Define $\mathbf{s}_M = \mathbf{F}\mathbf{x}_m$, the PSS detection can be performed as

$$\begin{aligned}\{\hat{M}, \hat{\theta}\} &= \arg\max_{M,\theta}\left\{\left|\mathbf{s}_M\left(\mathbf{y}_k^{(\theta)}\right)^H\right|^2\right\} \\ &= \arg\max_{M,\theta}\left\{\left|\mathbf{s}_M[0]\mathbf{y}_k^*[\theta] + \mathbf{s}_M[N/2]\mathbf{y}_k^*[\theta+N/2] + \Omega_{k,\theta}\right|^2\right\}, \end{aligned} \quad (4)$$

where $\mathbf{y}_k^{(\theta)} = [\mathbf{y}_k[\theta], \mathbf{y}_k[\theta+1], \cdots, \mathbf{y}_k[\theta+N-1]]^T$, and $\Omega_{k,\theta} = \sum_{n=1}^{N/2-1} \mathbf{s}_M[n]\mathbf{y}_k^*[\theta+n] + \sum_{n=N/2+1}^{N-1} \mathbf{s}_M[n]\mathbf{y}_k^*[\theta+n]$.

[2]Frequency offset and channel estimation have been studied considerably (e.g., in [6]–[10]), and they are beyond the scope of this paper.

III. Almost Half-Complexity (AHC) Non-Coherent PSS Detection

Since the odd-length ZC sequences as well as their IDFT transforms are always central symmetric, i.e.,

$$\mathbf{s}_M[i] = \mathbf{s}_M[N-i], \quad i = 1, \cdots, N/2-1, \quad (5)$$

$\Omega_{k,\theta}$ can be simplified as

$$\Omega_{k,\theta} = \sum_{n=1}^{N/2-1} \mathbf{s}_M[n]\left(\mathbf{y}_k[\theta+n] + \mathbf{y}_k[\theta+N-n]\right)^*. \quad (6)$$

Only $(N/2+1)$ complex conjugate multiply operations are required in (6). Since the complex conjugate multiply operations dominate the complexity of the PSS detection algorithms, almost one-half the complexity is saved in (6) as compared to (4) and, therefore, we call the proposed detector "Almost Half-Complexity (AHC)" algorithm.

IV. Central Self-Correlation (CSC)-based PSS Fast Detection

Although AHC reduces the computational complexity of PSS acquisition considerably, the complexity in each iteration is still too high, because the sequence root M should be identified for each θ. Although PSS is transmitted very infrequently (once per 5 ms period), the UE still needs to perform the PSS-detection aforementioned every time even if it is actually receiving a data symbol. This kind of operation really has a very low efficiency in terms of either power consumption or cell-search speed.

Thanks to the central-symmetric property of ZC sequences as well as their IDFT transforms, and also because this central-symmetric property always holds regardless of the exact M values, the PSS acquisition speed can be further simplified by exploiting ZC sequences' central self-correlation property[3]. Once a UE detects the central-symmetric pattern in the received vector, it means a PSS sequence is detected (without knowing the exact M value yet).

Like in [6], we define a timing metric of $\mathbf{y}_k$ as

$$\mathcal{Z}^{\mathrm{C}}(\theta) = \left|\sum_{n=1}^{N/2-1} \frac{\mathbf{y}_k[\theta+N-n]\cdot\mathbf{y}_k^*[\theta+n]}{|\mathbf{y}_k[\theta+N-n]\cdot\mathbf{y}_k^*[\theta+n]|}\right|^2. \quad (7)$$

The PSS can be identified at the UE by detecting the locally maximal $\mathcal{Z}^{\mathrm{C}}(\theta)$ value, and after a PSS is successfully detected, the UE will then identify the M value of the detected PSS.

[3]Frequency offset estimation in OFDM by exploiting the central-symmetric structure of training sequence has been studied in [6], [11], [12].

V. Frequency Offset Insensitive PSS Detection Based on the CSC Property (CSC_{Ins})

In both the conventional non-coherent detector and the proposed AHC and CSC algorithms, the timing metrics for PSS detection are always functions of frequency offset, and the best PSS detection performance is met at zero frequency offset. Once the normalized frequency offset approaches ± 1, these PSS detectors will totally fail.

In this section, we propose an improvement of CSC, i.e., CSC_{Ins}, to combat the large frequency offset. Notice that the frequency offset accumulation in $\lambda_{y,n}^{(\theta)} = \mathbf{y}_k[\theta+N-n]\cdot\mathbf{y}_k[\theta+n]$ is identical for each $n = 1, 2, \cdots, N/2-1$. Based on the received vector $\mathbf{y}_k$, let's first define a new vector $\boldsymbol{\lambda}_k^{(\theta)}$ as

$$\boldsymbol{\lambda}_k^{(\theta)} = \left[\lambda_{y,1}^{(\theta)}, \lambda_{y,2}^{(\theta)}, \cdots, \lambda_{y,\frac{N}{2}-1}^{(\theta)}\right]^T, \tag{8}$$

which converts the effect of the frequency offset into a common phase rotation. After that, let's define another local vector as

$$\mathbf{s}_{2M} = \mathbf{F}\left[\mathbf{0}_{\frac{N-62}{2}}, \mathbf{z}_{2M}, \mathbf{0}_{\frac{N-64}{2}}\right]^T, \tag{9}$$

where $\mathbf{z}_{2M}[n] = \exp\left[\dfrac{-\jmath\pi 2Mn(n+1)}{N_{ZC}}\right]$. The PSS detector CSC_{Ins} can be derived as

$$\{\hat{M}, \hat{\theta}\} = \arg\max_{M,\theta}\left\{\left|\tilde{\mathbf{s}}_{2M}^H \boldsymbol{\lambda}_k^{(\theta)}\right|^2\right\}, \tag{10}$$

where

$$\tilde{\mathbf{s}}_{2M} = \left[\mathbf{s}_{2M}[1], \mathbf{s}_{2M}[2], \cdots, \mathbf{s}_{2M}\left[\frac{N}{2}-1\right]\right]^T. \tag{11}$$

VI. Performance Analysis of the Proposed PSS Detection Algorithms

In the PSS searching process, a suitable threshold can be used by the UE to identify an appearing PSS successfully while at the same time minimizing the mistake of identifying a non-PSS symbol as PSS just because of the high interference and/or noise level. Therefore, a tradeoff between the False-Alarm probability (P_{FA}) and Miss-Detection probability (P_{MD}) is met.

For a given P_{FA}, the threshold of the AHC detector, i.e., $\mathcal{T}_{\text{Threshold}}^{\text{AHC}}$, can be derived as

$$\mathcal{T}_{\text{Threshold}}^{\text{AHC}} = N\sigma_w^2 \cdot \ln\left(\frac{1}{P_{FA}^{\text{AHC}}}\right). \tag{12}$$

Similarly, the threshold of CSC detector is derived as

$$\mathcal{T}_{\text{Threshold}}^{\text{CSC}} = \frac{(N-2)(2\sigma_w^2+\sigma_w^4)}{2} \cdot \ln\left(\frac{1}{P_{FA}^{\text{AHC}}}\right). \tag{13}$$

A. Miss-Detection probability of AHC

Define the AHC detector $\mathcal{Z}^{\text{A}}(\theta) = \left|\mathbf{s}_M^H \mathbf{y}_k^{(\theta)}\right|^2$. From [13, Chapter 2, Page 44], the expectation of $\mathcal{Z}^{\text{A}}(\theta)$ is derived as

$$\mathbb{E}\left\{\mathcal{Z}^{\text{A}}(\theta)\right\} = \frac{\sin^2 \pi\varepsilon}{\sin^2 \frac{\pi\varepsilon}{N}} + N\sigma_w^2, \tag{14}$$

where the subscript of ε is removed for brevity.

For a given threshold $\mathcal{T}_{\text{Threshold}}^{\text{AHC}}$, the probability that $\mathcal{Z}^{\text{A}}(\theta)$ being not larger than $\mathcal{T}_{\text{Threshold}}^{\text{AHC}}$, i.e., P_{MD}^{AHC}, is derived as

$$\begin{aligned} P_{MD}^{\text{AHC}} &= \mathbb{P}_{\text{r}}\left\{\mathcal{Z}^{\text{A}}(\theta) \le \mathcal{T}_{\text{Threshold}}^{\text{AHC}}\right\} \\ &= 1 - \exp\left\{-\frac{\left(\alpha_{N,\varepsilon}^{\text{AHC}}\right)^2 + \left(\beta_{N,\varepsilon}^{\text{AHC}}\right)^2}{2}\right\} \cdot \xi_{N,\varepsilon}^{\text{AHC}}, \end{aligned} \tag{15}$$

where

$$\begin{aligned} \xi_{N,\varepsilon}^{\text{AHC}} &= \mathfrak{I}_0\left(\alpha_{N,\varepsilon}^{\text{AHC}}\beta_{N,\varepsilon}^{\text{AHC}}\right) \\ &\quad + \sum_{k=1}^{N-1}\left[\left(\frac{\beta_{N,\varepsilon}^{\text{AHC}}}{\alpha_{N,\varepsilon}^{\text{AHC}}}\right)^k + \left(\frac{\alpha_{N,\varepsilon}^{\text{AHC}}}{\beta_{N,\varepsilon}^{\text{AHC}}}\right)^k\right]\mathfrak{I}_k\left(\alpha_{N,\varepsilon}^{\text{AHC}}\beta_{N,\varepsilon}^{\text{AHC}}\right) \\ &\quad + \sum_{k=N}^{\infty}\left(\frac{\alpha_{N,\varepsilon}^{\text{AHC}}}{\beta_{N,\varepsilon}^{\text{AHC}}}\right)^k \mathfrak{I}_k\left(\alpha_{N,\varepsilon}^{\text{AHC}}\beta_{N,\varepsilon}^{\text{AHC}}\right), \end{aligned} \tag{16}$$

$\mathfrak{I}_k(\cdot)$ is the k-th order modified Bessel function of the first kind and can be represented as

$$\mathfrak{I}_k(x) = \sum_{m=0}^{\infty}\frac{(x/2)^{k+2m}}{m!\Gamma(m+k+1)} = \sum_{m=0}^{\infty}\frac{(x/2)^{k+2m}}{m!(m+k)!}, \quad x \ge 0, \tag{17}$$

with $(m+k)$ being a non-negative integer, $\alpha_{N,\varepsilon}^{\text{AHC}} = \left|\dfrac{\sin(\pi\varepsilon)}{\sin(\frac{\pi\varepsilon}{N})}\right| \cdot \sqrt{\dfrac{2}{\sigma_w^2}}$, $\beta_{N,\varepsilon}^{\text{AHC}} = \sqrt{\dfrac{2\mathcal{T}_{\text{Threshold}}^{\text{AHC}}}{\sigma_w^2}}$, and $\beta_{N,\varepsilon}^{\text{AHC}} > \alpha_{N,\varepsilon}^{\text{AHC}} > 0$.

B. Miss-Detection probability of CSC

Similar to (14), the expectation of $\mathcal{Z}^{\text{C}}(\theta)$ is derivation as

$$\mathbb{E}\left\{\mathcal{Z}^{\text{C}}(\theta)\right\} = \frac{\sin^2 \frac{\pi\varepsilon(N-2)}{N}}{\sin^2 \frac{2\pi\varepsilon}{N}} + \left(\frac{N}{2}-1\right)\cdot\left(2\sigma_w^2+\sigma_w^4\right). \tag{18}$$

For a given threshold $\mathcal{T}_{\text{Threshold}}^{\text{CSC}}$, the Miss-Detection probability is derived as

$$\begin{aligned} P_{MD}^{\text{CSC}} &= \mathbb{P}_{\text{r}}\left\{\mathcal{Z}^{\text{C}}(\theta) \le \mathcal{T}_{\text{Threshold}}^{\text{CSC}}\right\} \\ &= 1 - \exp\left\{-\frac{\left(\alpha_{N,\varepsilon}^{\text{CSC}}\right)^2 + \left(\beta_{N,\varepsilon}^{\text{CSC}}\right)^2}{2}\right\} \cdot \xi_{N,\varepsilon}^{\text{CSC}}, \end{aligned} \tag{19}$$

TABLE I

SIMULATION PARAMETERS FOR THE CONVENTIONAL ALGORITHM, AHC AND CSC WITH $M = 25, 29, 34$ FOR PSS1, PSS2, PSS3, RESPECTIVELY.

Parameter	Scenario	Cell1	Cell2	Cell3	Unit
Relative Delay of 1st path	Syn.	0	0	Half CP	ms
	Asyn.	0	1.5	3	ms
PSS Physical Layer ID		PSS1	PSS2	PSS3	
		PSS1	PSS2	PSS1	
Objective Cell		Yes	No	No	

where

$$\xi_{N,\varepsilon}^{\text{CSC}} = \Im_0\left(\alpha_{N,\varepsilon}^{\text{CSC}}\beta_{N,\varepsilon}^{\text{CSC}}\right) + \sum_{k=1}^{N-1}\left[\left(\frac{\beta_{N,\varepsilon}^{\text{CSC}}}{\alpha_{N,\varepsilon}^{\text{CSC}}}\right)^k + \left(\frac{\alpha_{N,\varepsilon}^{\text{CSC}}}{\beta_{N,\varepsilon}^{\text{CSC}}}\right)^k\right]\Im_k\left(\alpha_{N,\varepsilon}^{\text{CSC}}\beta_{N,\varepsilon}^{\text{CSC}}\right) + \sum_{k=N}^{\infty}\left(\frac{\alpha_{N,\varepsilon}^{\text{CSC}}}{\beta_{N,\varepsilon}^{\text{CSC}}}\right)^k\Im_k\left(\alpha_{N,\varepsilon}^{\text{CSC}}\beta_{N,\varepsilon}^{\text{CSC}}\right), \tag{20}$$

with $\alpha_{N,\varepsilon}^{\text{CSC}} = \left|\frac{\sin\frac{\pi\varepsilon(N-2)}{N}}{\sin\frac{2\pi\varepsilon}{N}}\right| \cdot \sqrt{\frac{2}{2\sigma_w^2+\sigma_w^4}}$, $\beta_{N,\varepsilon}^{\text{CSC}} = \sqrt{\frac{2\mathcal{T}_{\text{Threshold}}^{\text{CSC}}}{2\sigma_w^2+\sigma_w^4}}$, and $\beta_{N,\varepsilon}^{\text{CSC}} > \alpha_{N,\varepsilon}^{\text{CSC}} > 0$.

C. Miss-Detection probability of CSC_{Ins}

Define the timing metric of CSC_{Ins} as $\mathcal{Z}^{\text{C}_{\text{Ins}}}(\theta) = \left|\tilde{\mathbf{s}}_{2M}^H\boldsymbol{\lambda}_k^{(\theta)}\right|^2$, the expectation of $\mathcal{Z}^{\text{C}_{\text{Ins}}}(\theta)$ can be derived as

$$\mathbb{E}\left\{\mathcal{Z}^{\text{C}_{\text{Ins}}}(\theta)\right\} = \left(\frac{N}{2}-1\right)\cdot\left(2\sigma_w^2+\sigma_w^4+1\right). \tag{21}$$

For a given threshold $\mathcal{T}_{\text{Threshold}}^{\text{CSC}_{\text{Ins}}}$, the Miss-Detection probability is derived as

$$P_{MD}^{\text{CSC}_{\text{Ins}}} = \mathbb{P}_{\text{r}}\left\{\mathcal{Z}^{\text{C}_{\text{Ins}}}(\theta) \le \mathcal{T}_{\text{Threshold}}^{\text{CSC}_{\text{Ins}}}\right\} = 1 - \exp\left\{-\frac{\left(\alpha_{N,\varepsilon=0}^{\text{CSC}}\right)^2+\left(\beta_{N,\varepsilon=0}^{\text{CSC}}\right)^2}{2}\right\}\cdot\xi_{N,\varepsilon=0}^{\text{CSC}}. \tag{22}$$

VII. NUMERICAL RESULTS

In this section, the performance of the proposed PSS detection algorithms is evaluated. The detailed simulation parameters are given by Table I. A three-cell environment is considered, with cell #1 being the objective cell and cell #2&#3 acting as the interfering ones. By considering the effect of signal propagation large-scale path loss, the UE receives power from cell #1 is 4.89 dB hgher than that from cell #2, and 5.93 dB higher than that from cell #3. Scenarios of both synchronous and asynchronous eNodeBs are analyzed, and the channel model used in [2] is considered here. The other simulation parameters follow the scenario defined in [14].

Timing metric for the conventional and the proposed detectors as functions of normalized frequency offset are shown in Fig. 1, where P_{FA} is set to be 10^{-3}. The working range of the conventional detector as well as the proposed AHC algorithm in terms of normalized frequency offset is (-0.74, 0.74). As compared to them, a relatively smaller working range, i.e., (-0.56, 0.56), is met for the proposed CSC detector. The most robust detector in terms of frequency offset combating capability is the proposed CSC_{Ins} detector, whose performance is independent of the frequency offset.

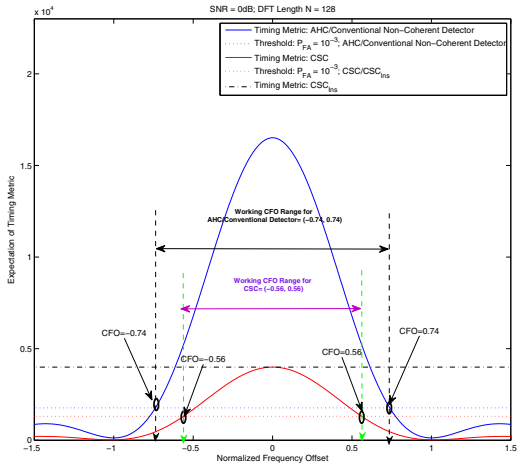

Fig. 1. Expectation of timing metric of the conventional non-coherent detector, the proposed AHC, CSC and CSC_{Ins}, respectively, as a function of normalized frequency offset.

Simulations about the performance comparison among the conventional and the proposed detectors in terms of 90% PSS acquisition time are performed, as numerical results being shown in Fig. 2, where the normalized frequency offset is set to be 0.1 (corresponding to 1.5kHz). AHC achieves exactly the same accuracy as that obtained in the conventional non-coherent algorithm. The accuracy of CSC algorithm is sacrificed to some extent for the considerable complexity gain. We also notice that in the CSC algorithm, its PSS detection performance in the synchronous scenario is always better than that obtained in the asynchronous scenario. We can explain this finding as follows: In the asynchronous transmission scenario, PSS transmitted by the objective cell will be affected by the data symbols from the interfering cells, and this kind of interference will definitely degrade the SINR of the received PSS. However, for the synchronous transmission scenario, PSSs transmitted from different cells may overlapped together and received by a single UE simultaneously, and, therefore, the CSC detection performance may be improved by an add-up effect of PSS signals.

Fig. 3 illustrates the PSS detection performance of the proposed CSC_{Ins} detector. A much shorter 90% PSS acquisition time compared to the other detectors is obtained in the CSC_{Ins} detector. Similar to the CSC detector, the CSC_{Ins} detector also obtains a relatively better performance in the synchronous interference scenario than that obtained in the asynchronous

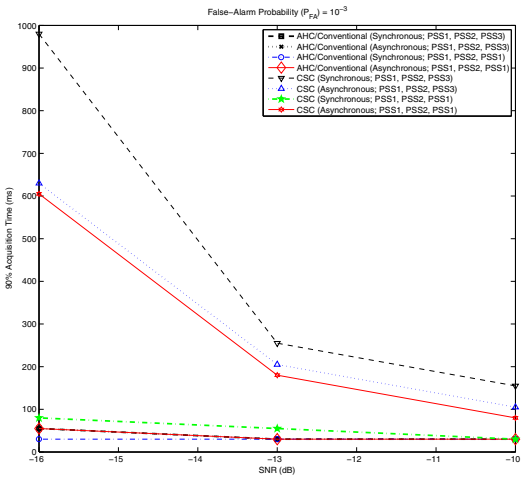

Fig. 2. The 90% PSS acquisition time comparison among the conventional, the AHC and the CSC algorithms with normalized frequency offset 0.1 and PSS1, PSS2, PSS3 being defined as ZC sequences rooted by $25, 29, 34$, respectively.

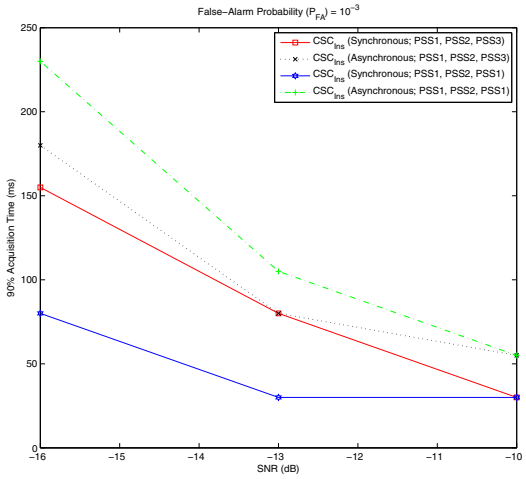

Fig. 3. The 90% PSS acquisition time for the proposed CSC_{Ins} algorithm with normalized frequency offset 0.1 and PSS1, PSS2, PSS3 being defined as ZC sequences rooted by $25, 29, 34$, respectively.

interference environment. For the synchronous interference environment, the PSS acquisition time obtained in the scenario of (PSS1, PSS2, PSS1) will be shorter than that obtained in the scenario of (PSS1, PSS2, PSS3), because of the add-up effect of the interfering PSS to the objective PSS.

VIII. Conclusions

The high-performance PSS detection algorithms for LTE system were discussed. Central-symmetric structure in the ZC sequence were exploited to improve the PSS detection performance. Both the proposed AHC and CSC detectors outperforms the conventional non-coherent detector in terms of complexity reduction. An improvement of CSC detector, i.e., CSC_{Ins}, was also proposed to improve the frequency offset combating capability. All the proposed detectors work well in a low-SNR regime, and as compared to the conventional detector, the proposed CSC and CSC_{Ins} detectors are more suitable for working in a synchronous-interference scenario due to their utilization of ZC sequence's central-symmetric property. A fast PSS acquisition with the 90% acquisition time of 55ms can be achieved in the proposed CSC detector at the SNR of -10 dB, and this acquisition time can be further reduced to 30ms if the proposed CSC_{Ins} detector is applied.

References

[1] J. D. C. Chu, "Polyphase codes with good periodic correlation ptoperties," *IEEE Trans. Inform. Theory*, vol. 18, pp. 531–532, July 1972.

[2] I. T. S. Sesia and M. Baker, *LTE - The UMTS Long Term Evolution: From Theory to Practice*. New York: John Wiley & Sons, 2009.

[3] 3GPP TS 36.211 v8.5.0, "Technical Specification Group Radio Access Network: Evolved Universal Terrestrial Radio Access (E-UTRAN)," Physical channels and modulation (Release 8).

[4] V. J. W. X. K. Manolakis, D. M. G. Estevez and C. Drewes, "A closed concept for synchronization and cell search in 3GPP LTE systems," in *IEEE Wireless Commun. and Networking Conf.*, Budapest, Hungary, Apr. 2009.

[5] W. Xu and K. Manolakis, "Robust synchronization for 3GPP LTE systems," in *IEEE Global Telecommn. Conf. (GLOBECOM)*, Miami, FL, 2010.

[6] Z. Zhang, K. Long, M. Zhao, and Y. Liu, "Joint frame synchronization and frequency offset estimation in OFDM systems," *IEEE Trans. Broadcast*, vol. 51, no. 3, pp. 389–394, Sept. 2005.

[7] M. Movahhedian, Y. Ma, and R. Tafazolli, "Blind CFO estimation for linearly precoded OFDMA uplink," *IEEE Trans. Signal Processing*, vol. 58, no. 9, pp. 4698–4710, Sept. 2010.

[8] H. Mehrpouyan and S. D. Blostein, "Bounds and algorithms for multiple frequency offset estimation in cooperative networks," *IEEE Trans. Wireless Commun.*, vol. 10, no. 4, pp. 1300–1311, Apr. 2011.

[9] R. Corvaja and A. G. Armada, "SINR degradation in MIMO-OFDM systems with channel estimation errors and partial phase noise compensation," *IEEE Trans. Commun.*, vol. 58, no. 8, pp. 2199–2203, Aug. 2010.

[10] Z. Zhang, W. Jiang, H. Zhou, Y. Liu, and J. Gao, "High accuracy frequency offset correction with adjustable acquisition range in OFDM systems," *IEEE Trans. Wireless Commun.*, vol. 4, no. 1, pp. 228–237, Jan. 2005.

[11] Z. Zhang, M. Zhao, H. Zhou, Y. Liu, and J. Gao, "Frequency offset estimation with fast acquisition in OFDM system," *IEEE Commun. Lett.*, vol. 8, no. 3, pp. 171–173, Mar. 2004.

[12] Z. Zhang, H. Kayama, and C. Tellambura, "New joint frame synchronisation and carrier frequency offset estimation method for OFDM systems," *Euro. Trans. Telecommun.*, vol. 20, no. 4, pp. 413–430, June 2009.

[13] J. G. Proakis, *Digital Communications*, 4th ed. McGraw-Hill, 2001.

[14] M. E. Texas Instruments, NXP and Nokia, "R4-072215: Simulation assumptions for intra-frequency cell identification," *www.3gpp.org 3GPP TSG RAN WG4, meeting 45, Jeju, Korea*, 2007.

Acknowledgement

This work was supported by the National Basic Research Program of China (2012CB315905), the National Natural Science Foundation of China (61172050, 61172048, 61100184, and 61173149), National Key Projects, Beijing Science and Technology Program, Chang Jiang Scholars Program of the Ministry of Education of China, Program for New Century Excellent Talents in University, and NEC China Research Foudation. The corresponding Author is Dr. Keping Long.